International Journal of Industrial Electronics, Control and Optimization © 2020 IECO
Vol. 3, No. 4, pp. 483-490, Sep (2020)

Optimal Impedance Voltage-Controller for Electrically Driven Robots

Mohsen Jalaeian F. [1,†], Mohammad Mehdi Fateh[2], and Morteza Rahimiyan[3],

[1,2,3] Department of Electrical and Robotic Engineering, Shahrood University of Technology, Shahrood, Iran,

ABSTRACT

This paper presents a novel optimal impedance voltage-controller for Electrically Driven Lower Limb Rehabilitation Robots (EDLR). To overcome the dynamical complexities, and handle the uncertainties, the proposed method employs an expected forward model of the actuator. The existing value of lamped uncertainty is represented by the output difference of the model and system. A voltage-controller, which compensates for the uncertainties, is designed based on this uncertainty estimator. Parameters of the controller are optimized using genetic algorithms. Key contributions of this paper are I) uncertainty estimation through the expected model's output, II) overcoming the changes in motors' parameters, III) introducing a class of closed-loop system termed as "Repeatable", and IV) designing an optimal impedance voltage-controller that is non-sensitive to the parameter variations. Significant merits of the approach are swift calculations, efficiency, robustness, and guaranteed stability. Furthermore, the simplicity of design, ease of implementation and model-free independent joint structure of the approach are noticeable. The method is compared with an adaptive robust sub-controller and a Taylor-series-based adaptive robust controller, through simulations in passive range of motion and active assistive rehabilitation exercises. The results show the superiority of the proposed method in tracking performance and the time of calculations.

Article Info

Keywords:
Electrically Driven Robots (EDR), Impedance control, Model-free tracking control, Rehabilitation robots, Voltage-based control,

Article History:
Received: 2020-02-03
Accepted: 2020-04-19

I. INTRODUCTION

The human lower limb's dysfunctionality has significant effects on daily life quality [1]. Nowadays, patients suffering from such diseases may improve their lower limb motor function through robotic rehabilitation programs [2]. Robots provide several benefits for the therapeutic process, namely reducing the costs [3], speeding up the process [4], reducing pain [5], as well as being user-friendly [6]. However, control of rehabilitation robots is a difficult complex problem, due to the lack of an accurate model for the human body, and the high sensitivity to interconnection forces [7]. In addition, the Electrically Driven Robots (EDR), has coupled third-order nonlinear differential equations [8]. Moreover, since the robot may be powered by batteries, energy consumption is another important issue.

Over the last decade, in the field of therapeutic robots' control, several scientific articles such as a PID [9], adaptive robust controller [10], as well as voltage-based adaptive control [11] are presented.

In terms of using system equations, robot control methods are divided into four categories: (i) Model Free Controllers (MFC) [9], (ii) Computed Torque Control (CTC) [12], (iii) Integrated Dynamics Methods (IDM) [8], and (iv) Voltage Control Strategy (VCS) [11,13,14]. Although the robot control signal is applied through the actuators, they are not considered in the MFC and CTC methods. The IDMs have heavy time-consuming calculations, whereas the dynamic effects of the complex coupled nonlinear dynamics of the robot, environment, and the mechanical part of the motor, altogether are observable in the motor current. Thus, the VCS methods design the controller using the electrical portion of

[†]Corresponding Author : m.jalaeian@yahoo.com
Faculty of Electrical and Robotic Engineering, Shahrood University of Technology, Shahrood, Iran

the actuator's dynamics [13]. However, the electrical current's derivative is hard to be measured [15,16], and actuator parameters may vary due to heat [17]. The VCS strategies try to approximate, estimate, or predict the unmeasurable parts of the equation using different types of observers or approximators. To do so, an adaptive uncertainty estimator [8], an adaptive impedance approach [11], fuzzy approximators [14,18,19], an estimator based on Fourier series expansion [16], a FAT-based robust adaptive approximator [20], and a Taylor series approximator [21] are introduced.

To the best of our knowledge, the variation of motor parameters is neglected in the literature. To overcome these challenges, a novel voltage-controller is proposed in this research that uses the known part of the system to estimate the model imperfection. In [22], a forward internal model is used to control a lower extremity exoskeleton; however, since it utilizes the dynamical model of the robot, the final control law is a complex highly nonlinear coupled system. In this paper, we employ the VCS to reach a simple final controller. The advantages of the approach are swift calculations, fast response, efficiency, guaranteed closed-loop stability, simplicity of design, ease of implementation, and independent joint structure.

This paper includes the following sections: Section 2 is allocated to detail the dynamical model of the EDLR. The proposed method is described in Section 3 while the analysis of its stability is expressed in Section 4. Then, the description and analysis of the simulations and comparisons are detailed in Section 5. Finally, the paper is concluded in the last section.

II. MODEL OF AN EDLR

The EDLR (Fig. 1) is a robot, with two degrees of freedom, which is used to provide rehabilitation exercises for the human lower limb in the sagittal plane [2,4].

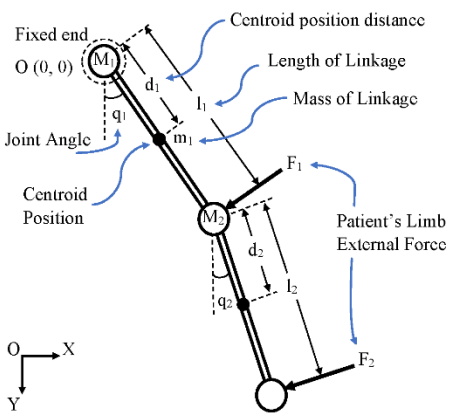

Fig. 1. The EDLR, assembly drawing.

The equations of motion of an EDLR can be written as Equ. (1), [10]. In this paper, the matrices and vectors are written in bold characters while the scalars are written in narrow fonts.

$$\boldsymbol{M}(\boldsymbol{q})\ddot{\boldsymbol{q}} + \boldsymbol{H}(\boldsymbol{q},\dot{\boldsymbol{q}}) + \boldsymbol{J}(\boldsymbol{q})^T\boldsymbol{F_e} + \boldsymbol{d} = \boldsymbol{T_r} \quad (1)$$

in which, $\boldsymbol{q} = [q_1, q_2, \dots, q_n]^T$ is the vector of joints angles, where n is the robot's degree of freedom, $\boldsymbol{M}(\boldsymbol{q}) \in \mathbb{R}^{n\times n}$ is inertia matrix, $\boldsymbol{H}(\boldsymbol{q},\dot{\boldsymbol{q}}) \in \mathbb{R}^{n\times 1}$ is a vector containing the centripetal, Coriolis, and gravity forces, $\boldsymbol{J}(\boldsymbol{q})$ is the Jacobian matrix of the robot, $\boldsymbol{F_e} \in \mathbb{R}^{n\times 1}$ is a vector representing the patient-exerted-forces, $\boldsymbol{T_r}$ is the joints torques vector, and $\boldsymbol{d}$ is the lumped bounded uncertainty. The torque of i^{th} joint is produced by an electrical DC motor through a gearbox with the speed transmission ratio of r_i, that means:

$$\dot{q}_i = r_i\dot{\theta}_i \quad (2)$$

in which, $\dot{\theta}_i$ is the angular speed of the motor shaft. The dynamic equations of each DC motor consist of two parts, namely a mechanical portion and an electrical equation.

$$J_{m,i}\ddot{\theta}_i + B_{m,i}\dot{\theta}_i + r_iT_{r,i} = K_{m,i}I_i \quad (3)$$

$$L_i\dot{I}_i + R_iI_i + K_{b,i}\dot{\theta}_i = V_i \quad (4)$$

where, $J_{m,i}$ and $B_{m,i}$ are the inertia and friction of the motor. V_i, I_i, and $T_{r,i}$ are the motor's terminal voltage, armature current, and joint torque, respectively. $K_{m,i}$ and $K_{b,i}$ are the motor torque transmission and back-EMF constants. L_i, and R_i are the actuator inductance and resistance.

The block diagram of a robotic-assisted lower limb rehabilitation process is depicted in Fig. 2.

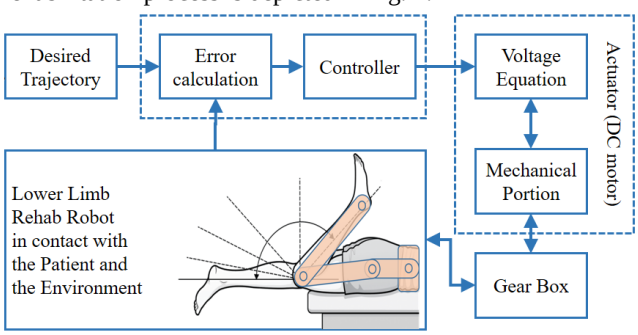

Fig. 2. Block-diagram of robotic rehabilitation.

Substituting Equs. (1)-(2) in Equ. (3), the integrated mechanical portion is obtained:

$$(\boldsymbol{r_M}\boldsymbol{M}(\boldsymbol{q}) + \boldsymbol{r_M}^{-1}\boldsymbol{J_M})\ddot{\boldsymbol{q}} + \boldsymbol{r_M}^{-1}\boldsymbol{B_M}\dot{\boldsymbol{q}} + \boldsymbol{r_M}\boldsymbol{H}(\boldsymbol{q},\dot{\boldsymbol{q}}) + \boldsymbol{r_M}\boldsymbol{J}(\boldsymbol{q})^T\boldsymbol{F_e} + \boldsymbol{r_M}\boldsymbol{d} = \boldsymbol{K_M}\boldsymbol{I} \quad (5)$$

in which, $\boldsymbol{J_M}, \boldsymbol{B_M}, \boldsymbol{K_M}$, and $\boldsymbol{r_M}$, are the diagonal matrices of the mechanical parameters of all motors.

Property 1 (Inertia Matrix Invertibility):

The $\boldsymbol{M}(\boldsymbol{q})$, is a symmetric positive definite matrix, which is bounded even if $\boldsymbol{q}$ is not bounded. Therefore, $\bar{\boldsymbol{M}}(\boldsymbol{q}) = (\boldsymbol{r_M}\boldsymbol{M}(\boldsymbol{q}) + \boldsymbol{r_M}^{-1}\boldsymbol{J_M})$ is a positive definite bounded matrix, and its inverse exists and remains non-zero and bounded [23].

Considering property 1, one can rewrite the dynamics of mechanical portion as:

$$\ddot{\boldsymbol{q}} = \bar{\boldsymbol{M}}(\boldsymbol{q})^{-1}\big(\boldsymbol{K_M I} - (\boldsymbol{r_M}^{-1}\boldsymbol{B_M}\dot{\boldsymbol{q}} + \boldsymbol{r_M H}(\boldsymbol{q},\dot{\boldsymbol{q}}) + \boldsymbol{r_M J}(\boldsymbol{q})^{T}\boldsymbol{F_e} + \boldsymbol{r_M d})\big) \quad (6)$$

Assumption 1 (Desired Trajectory):

The desired angular position ($\boldsymbol{q_d}$), velocity ($\dot{\boldsymbol{q}}_{\boldsymbol{d}}$), and acceleration ($\ddot{\boldsymbol{q}}_{\boldsymbol{d}}$) are given bounded.

Assumption 2 (Voltage Supplier):

The input voltage, which is produced by a real supplier, is bounded because of factual limits.

$$|\boldsymbol{V}| \le \boldsymbol{V_{max}} \quad (7)$$

Assumption 3 (Measurement Noises):

It is assumed that each measured signal is passed through a low-pass filter; thus, the measurement noise is not considered in the course of this paper.

III. The Proposed Position Controller

The voltage equation of each actuator is considered independently without losing generality. The subscript i is omitted, and $\alpha \triangleq K_b r^{-1}$ is defined for the sake of simplicity, hence, Equ. (4) can be rewritten as:

$$\alpha\dot{q} + L\dot{I} + RI = V \quad (8)$$

Based on Equ. (5), the motor current represents the dynamical effect of the entire mechanical parts of the system [13]. Therefore, Equ. (8) can be used to design the controller in an independent joint structure.

A. *Case 1: Expected-Model Voltage Control with fixed known parameters:*

Here, we consider a simple forward model of the system defined as:

$$\dot{\hat{q}}(t) = \alpha^{-1}\big(V(t-\varepsilon) - RI(t)\big) \quad (9)$$

The unknown portion of the system can be computed by attention to Equs. (8) and (9) as:

$$\psi(t) \triangleq \dot{\hat{q}}(t) - \dot{q}(t) \equiv \alpha^{-1}\left(L\dot{I}(t) - \delta(t)\right) \quad (10)$$

in which, $\delta(t) = \big(V(t) - V(t-\varepsilon)\big)$, and ε is a very small positive value as a time delay. Then, the control law can be designed as:

$$V = RI + \alpha(\dot{q}_d + \lambda e + \psi) \quad (11)$$

where, $e \triangleq q_d - q$, is the error of the joint angle, and λ is a real positive scalar. The tracking error dynamics, which is discussed later in details, is equivalent to $\dot{e} + \lambda e = \alpha^{-1}\delta(t)$.

B. Case 2: Extended-Model Voltage Control with parameters variations:

Motor parameters may vary during the runtime owing to the motor heat and temperature changes [17]. Hence, the parameters R and α are supposed to be unknown, and two suggested design parameters, $\hat{R}$ and $\hat{\alpha}$, are utilized, instead. The new model can be proposed as:

$$\dot{\hat{q}}(t) = \hat{\alpha}^{-1}\left(V(t-\varepsilon) - \hat{R}I(t)\right) \quad (12)$$

Using the new model, Equ. (12), total imperfection can be measured as:

$$\psi(t) \triangleq \dot{\hat{q}}(t) - \dot{q}(t) \quad (13)$$

Analytically, the imperfection term (ψ) equivalents:

$$\psi \equiv \alpha^{-1}\big(L\dot{I} + RI\big) - \hat{\alpha}^{-1}\hat{R}I - \xi \quad (14)$$

in which, $\xi = \big(\alpha^{-1}V(t) - \hat{\alpha}^{-1}V(t-\varepsilon)\big)$. Accordingly, a new control law is proposed as:

$$V(t) = \hat{R}I + \hat{\alpha}(\dot{q}_d + \lambda e + \psi) \quad (15)$$

Applying the proposed control law, Equ. (15), to the electrical equation of the actuator, Equ. (8), yields:

$$\dot{q} = \alpha^{-1}\left(\big(\hat{R}I + \hat{\alpha}(\dot{q}_d + \lambda e + \psi)\big) - L\dot{I} - RI\right) \quad (16)$$

For analyzing the closed-loop system, the imperfection term, ψ, can be substituted with its analytical equivalence, Equ. (14):

$$\alpha\dot{q} = \hat{\alpha}(\dot{q}_d + \lambda e) + \hat{R}I - \big(L\dot{I} + RI\big) + \hat{\alpha}\big(\alpha^{-1}\big(L\dot{I} + RI\big) - \hat{\alpha}^{-1}\hat{R}I - \xi\big) \quad (17)$$

That yields:

$$(\dot{e} + \lambda e) = (\hat{\alpha}^{-1}\alpha - 1)\dot{q} + (\hat{\alpha}^{-1} - \alpha^{-1})\big(L\dot{I} + RI\big) + \xi \quad (18)$$

Apply some manipulations and exchanging ξ, we obtain:

$$(\dot{e} + \lambda e) = (\hat{\alpha}^{-1} - \alpha^{-1})\big(\alpha\dot{q} + L\dot{I} + RI\big) + \big(\alpha^{-1}V(t) - \hat{\alpha}^{-1}V(t-\varepsilon)\big) \quad (19)$$

Considering Equ. (8), we have:

$$(\dot{e} + \lambda e) = \hat{\alpha}^{-1}\big(V(t) - V(t-\varepsilon)\big) \quad (20)$$

Thus, the closed-loop system can be represented by:

$$(\dot{e} + \lambda e) = \hat{\alpha}^{-1}\delta(t) \quad (21)$$

Note that, although $\hat{\alpha}$ is noticed in Equ. (21), the estimation errors, $\tilde{R} \triangleq \big(R - \hat{R}\big)$ and $\tilde{\alpha} \triangleq (\alpha - \hat{\alpha})$, do not play any role in the closed-loop system. The pseudo-code of the proposed algorithm is detailed in Fig. 3.

- Initialize the control parameters ($\hat{R}$ *and* $\hat{\alpha}$)
- Initialize the imperfection indicator ($\psi = 0$)
- While (time < final_time)
  - Compute the control signal (V)
  - Apply recent control signal into the system
  - Measure the feedback variables (I *and* $\dot{q}$)
  - Compute the forward model output ($\dot{\hat{q}}$)
  - Compute the imperfection indicator (ψ)
- End While

Fig. 3. The proposed controller pseudo-code.

In a rehabilitation robot with revolute joints driven by DC motors with bounded terminal voltages, the electrical current, its derivative, and the angular velocity remain bounded [11]. The closed-loop system stability is studied here. According to assumption 2, $V(t)$ is bounded. When voltage is saturated, $|V| = V_{max}$, it can be concluded that $\delta(t) = 0$, and it leads the Equ. (21) to become $\dot{e} + \lambda e = 0$. If the voltage is not saturated, $|V| < V_{max}$, then $|\delta(t)| < 2V_{max}$, and consequently, the input value of Equ. (21) is bounded.

Therefore, the boundedness of error, e, and its derivative, $\dot{e}$, are guaranteed [24]. Thus, according to assumption 1, the actual position and velocity of the joint, $(q, \text{and } \dot{q})$, and of the motor, $(\theta, \text{and } \dot{\theta})$, remain bounded as well. Having assumption 2 and equation (8), the following is gained:

$$L\dot{I} + RI = v \tag{22}$$

in which $v = (V - \alpha\dot{q})$ is a bounded value as proved. Since Equ. (22) is a first-order linear differential equation with positive-constant coefficients, it is stable based on the Routh-Hurwitz criterion. With bounded input, v, the responses $(I, \text{and } \dot{I})$ are bounded [24]. Although the motor parameters vary during time, they are always positive and bounded due to physical constraints. Ergo, Equs. (12) and (13) claim that $\hat{\dot{q}}$ and ψ are bounded. In addition, Equ. (3) shows that the produced joints torque, $\boldsymbol{T_r}$, is bounded. So, the closed-loop system is stable. □

IV. Proposed Impedance Control, Design, and Optimization

The main idea of mechanical impedance control is to enhance the desirability of dynamical interactions between a robot and its environment [25,26]. The desired impedance law for each joint is defined as a second order equation [7].

$$M_d(\ddot{q}_d - \ddot{q}_r) + B_d(\dot{q}_d - \dot{q}_r) + K_d(q_d - q_r) = J(q)^T F_e \tag{23}$$

in which, $M_d, B_d, \text{and } K_d$ are the desired inertia, damping, and stiffness, respectively, and q_d is the desired trajectory. In addition, q_r is a regenerated trajectory for the joint angle based on the desired impedance law, which is obtained as:

$$\ddot{q}_r = \ddot{q}_d + {M_d}^{-1}[B_d(\dot{q}_d - \dot{q}_r) + K_d(q_d - q_r) - J(q)^T F_e] \tag{24}$$

Since $F_e, q_d, \dot{q}_d$ and $\ddot{q}_d$ are bounded, and the desired impedance coefficients are positive, the q_r is bounded. The block diagram of the proposed impedance control is presented in Fig. 4.

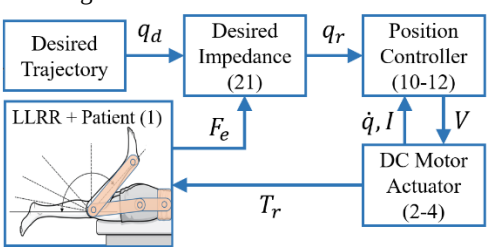

Fig. 4. The block-diagram of using impedance controller in rehabilitation.

Successful uncertainty handling is one of the main advantages of the proposed method, which enables the designer to tune the controller parameters using an offline optimization algorithm, like Genetic Algorithms (GAs) or Particle Swarm Optimization (PSO) [15,23]. Here, this characteristic is termed as "repeatability" of the closed-loop control system.

Definition 1: Repeatable closed-loop system

A closed-loop system is termed "*Repeatable*" if a fixed set of controller-parameters leads to a repetitive closed-loop response, even in the presence of uncertainty and external disturbances. In other words, in a repeatable closed-loop system:

$$\int_0^t \left(e(\tau) - e(\tau|\langle\phi, d\rangle)\right)^2 d\tau \ll \int_0^t \left(e(\tau)\right)^2 d\tau \tag{25}$$

where, $e(\tau)$ is the tracking error of the closed-loop system without uncertainty or external disturbances, and $e(\tau|\langle\phi, d\rangle)$ is the tracking error of the closed-loop system in the presence of model uncertainty, (ϕ), and external disturbances, (d), and $\langle . \rangle$ is used to denote the expectation value of the variables.

Remark 1:

Offline techniques are not being able to optimize the controller-parameters, due to the erratic essence of the system response, in the case of the unrepeatable system. However, if a system is repeatable, the offline optimization algorithm can be used to optimize its parameters; while uncertainties and unknown external disturbances have neglectable impacts on the results.

Remark 2:

The EDR with the proposed controller is repeatable, thus, the offline techniques may be utilized to optimize its parameters, without any worries about the exposure to uncertainty and external disturbances.

V. Simulations

In this section, two simulation scenarios (comparative position control, and optimized impedance control) of the LLRR are studied, in which, MATLAB® 2018a software is utilized within an ASUS laptop powered by Windows 10, and an Intel® Core™ i7-2.6GH CPU.

A. Position Control:

The proposed controller is applied to a 2-DoF EDLR for hip and knee therapeutic exercises. Human joints have a certain Range of Motion (ROM), which are considered inside the interval of (-30˚, +120˚) for hip and (-90˚,0˚) for knee, [10,28,29]. In addition, Maximum Angular Speeds (MAS) of hip and knee joints are considered equal to 30 degrees per second. The parameters of motor and robot are detailed in Table 1. Interested readers can find full details of the dynamic equations in [10]. The proposed controller is applied to the position control in comparison with two other controllers, namely an adaptive robust sub-controller (ARSC) [10], and a Taylor-series-based adaptive robust controller (TSARC) [8].

TABLE I
PARAMETERS OF ELECTRICALLY DRIVEN LLRR

Parameter	Dimension	Joint 1	Joint 2
$\boldsymbol{m_i}$	kg	5.5	5
$\boldsymbol{l_i}$	m	0.5	0.45
$\boldsymbol{d_i}$	m	0.45	0.4
$\boldsymbol{I_i}$	$kg.m^2$	0.25	0.2
$\boldsymbol{F_s}$	$N.m$	0.9	0.9
$\boldsymbol{F_c}$	$N.m$	0.8	0.8
σ_i	$N.m/rad.s^{-1}$	1.2	1.2
K_m	$N.m/A$	4.32	4.32
R_i	Ω	4	4
L_m	H	2.5e-3	2.5e-3
K_v	$v/rad.s^{-1}$	0.287	0.287
$K_g = r^{-1}$	-	16	16

Remark 3:

In order to perform a Passive ROM exercise for lower limb rehabilitation in the joint training practice, previous scientific works set the desired joint trajectory as a four-part piecewise linear periodic path, which is very simple but not smooth [9,10], or as a sinusoidal trajectory, which has not enough rest in each period for the patient. This study proposes an adjustable smooth and continuous trajectory whose derivative is computable analytically. Thus, the angular position and speed are desirably adjustable. Since the exercises are periodic, the time inside each period is defined as $\eta = Rem\left(\frac{time}{T_{prd}}\right)$, in which T_{prd} is a pregiven cycle-time that is determined by the physiotherapist, and $Rem(.)$ computes the reminder value of the division. Afterward, the desired trajectory is proposed based on the η.

$$q_d(\eta) = \big(max(ROM) - min(ROM)\big) \times \big(y(\eta,\eta_1) - y(\eta,\eta_2)\big) + min(ROM) \quad (26)$$

where $y(\eta,\eta_i) = \left(1 + \exp\left(-\frac{\eta-\eta_i}{a}\right)\right)^{-1}$, and a is a setting parameter for maximum angular speed.

The desired trajectory, which is introduced in remark 3, is applied to the proposed position control method. The tracking performances of hip and knee joints are shown in Fig. 5.

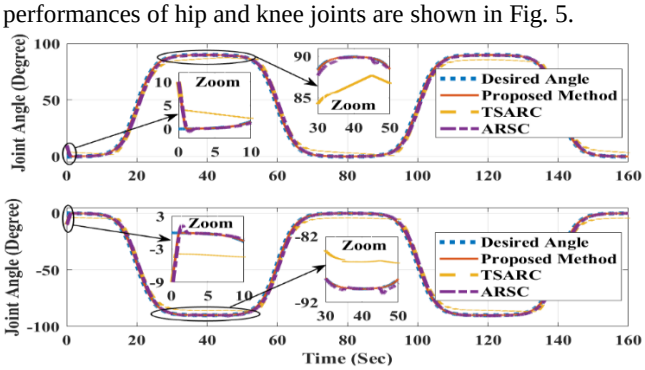

Fig. 5. PROM tracking performance of hip and knee joints.

According to Fig. 5, the proposed controller shows better tracking performance due to the smaller error and zero overshoot. There is an initial angle error that the controller overcomes it by nearly two seconds, (First zoomed areas in Fig. 5). To study the control performance, an external disturbance ($d = 2N$) is applied to the robot between the 35sec and 45sec, which the controller succeeds to damp its effects completely (Second zoomed areas in Fig. 5). Tracking errors are depicted in Fig. 6, where its value is small with the proposed controller, and the external disturbances do not affect the closed-loop errors (repeatability).

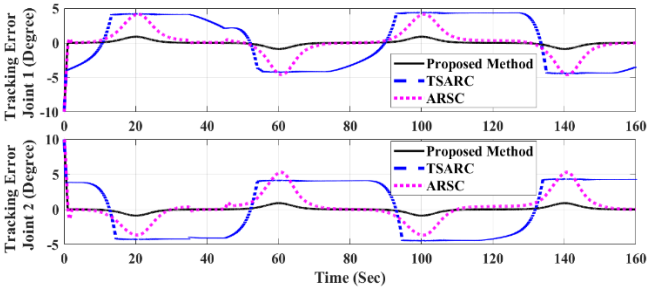

Fig. 6. PROM tracking error of hip and knee joints (comparison).

Based on Fig. 6, the proposed method proves superiority since its error magnitude is smaller than the other two, while no oscillation is observed in its response. To have a numerical comparison, several indices are studied in Table 2.

TABLE II
NUMERICAL COMPARISON

	Proposed Method		TSARC		ARSC	
Joint	**1**	**2**	**1**	**2**	**1**	**2**
ACT	1.22e-5		3.78e-5		1.60e-4	
MCT	2.21e-4		2.90e-3		4.2e-3	
MAV	2.778	2.785	3.956	3.973	2.850	3.100
MAC	0.66	0.26	0.82	0.49	0.68	0.28
SAE	8.68e2	8.78e2	5.8e4	6.1e4	1.9e4	2.1e4
MSE	0.21	0.21	7.39	7.61	3.53	4.01

ACT=Average cycle time, MCT=Max cycle time, MAV=Mean Absolute Voltage, MAC=Mean Absolute Current, SAE=Sum Absolute Error, MSE=Mean Square Error,

From the performance point of view, the tracking error of the proposed controller in both indices (Sum Absolute Error and Mean Square Error) is smaller than the other two. In addition, from the efficiency point of view, Mean Absolute Voltage, Mean Absolute Current and Average Cycle Time of the controller computation are studied while the proposed controller is better in those features. The proposed controller is superior in efficiency and performance, in spite of its great simplicity in design and implementation. Furthermore, the proposed structure is not sensitive to parameters estimation error. The controller has a few design parameters which should be set once in the first run. In contrast with a majority of controllers that have many design parameters and are sensitive to their setting values, which must be readjusted for each new trajectory. Control signals, the terminal voltages of motors, are illustrated in Fig. 7. As seen, the voltages are saturated when the error is big; however, the controller

overcomes and becomes unsaturated as fast as possible. The effect of external disturbance on voltages can be seen in the zoomed area in Fig. 7. Motors currents are displayed in Fig. 8 as well. Fig. 8 shows that the current is small and smooth. Based on the aforementioned principle, the dynamical behaviors of mechanical parts can be observed in the currents, as seen in Fig. 8.

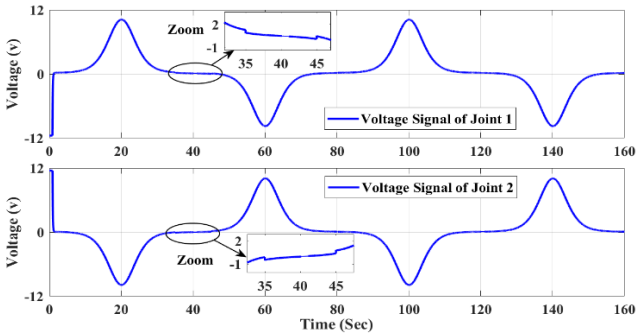

Fig. 7. motors voltages (control signals) of hip and knee joints.

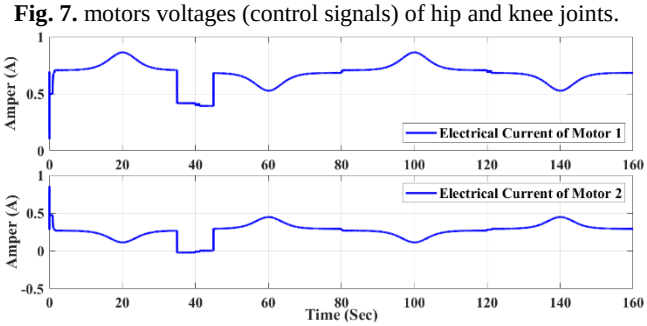

Fig. 8. DC motors currents.

B. Optimized Impedance Control:

The proposed scheme is utilized in impedance control of the LLRR in the presence of uncertainty and external disturbance. Based on remarks 1 and 2, GA is used to minimize the Mean Square Error (MSE) of tracking performance. Note that, the cost function for optimization can be selected based on error and energy [30], or one of them.

As expected, changes on $\hat{R}$ do not affect system performance. Nevertheless, the effect of changing in $\hat{\alpha}$ should be taken into account. Fig. 9 illustrates the impact of changes in $\hat{\alpha}$. The optimized $\hat{\alpha}$ is used, to minimize the error. Fig. 10 illustrates the patient's exerted force.

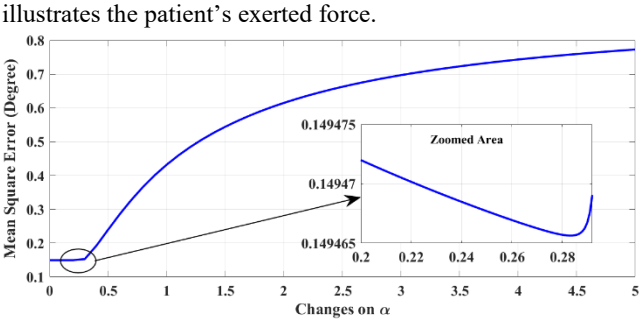

Fig. 9. The impact of changes in $\hat{\alpha}$ on impedance error.

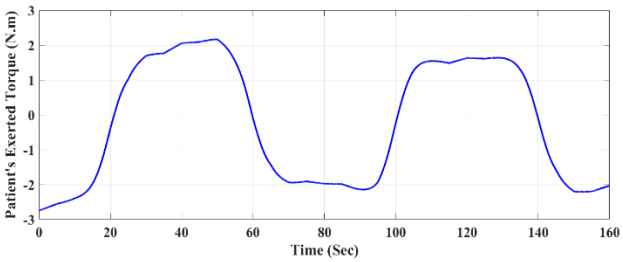

Fig. 10. Patient's exerted force.

The tracking performance is also depicted in Fig. 11, where the regenerated and actual trajectories are shown.

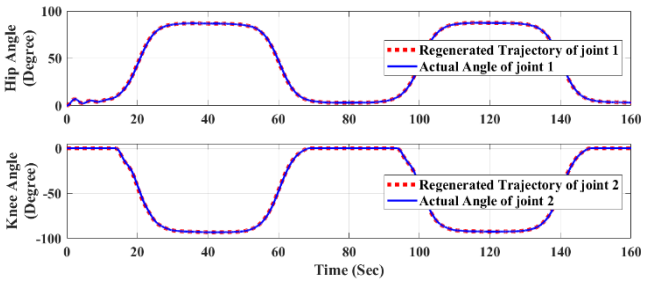

Fig. 11. Tracking performance (regenerated and actual trajectories).

Fig. 11 shows that the actual joints angles track the regenerated trajectories. However, the difference between them is shown in Fig. 12, as the impedance tracking error, with less than a few degrees which is neglectable in the context of rehabilitation.

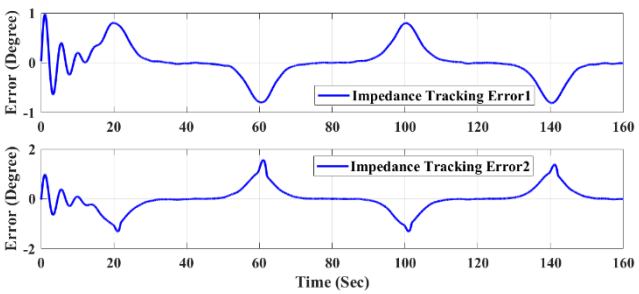

Fig. 12. The difference between the measured and commanded errors.

Applied voltages to the actuators are shown in Fig. 13.

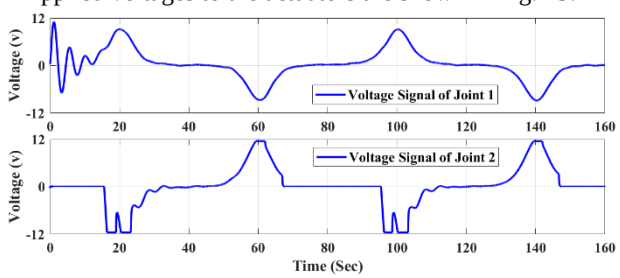

Fig. 13. Actuators' voltages (control signal).

These voltages provide the joints torques, which are depicted in Fig. 14.

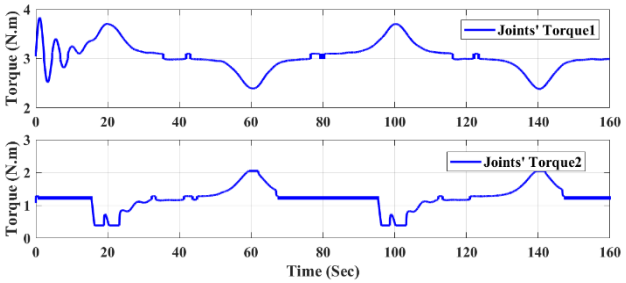

Fig. 14. Joint Torque.

It can be seen that the actuators' voltages are smooth and bounded. In other words, the closed-loop system that contains the robot, patient, and the environment, altogether behaves as the reference desired impedance rule.

In the future studies, authors going to utilize model predictive compensator or dynamic-growing fuzzy-neural acceleration-based compensator, which are first introduced by the authors in [31,32], to compensate for the effects of $\delta(t)$.

VI. Conclusions

The EDLRs can be controlled through the terminal voltage of their actuators in an independent joint manner. However, the parameters of actuators may vary over time and the value of the motor current derivative is unmeasurable. In this paper, a novel approach has been proposed to overcome these challenges. The proposed control method, which is applied to the position and optimal impedance control of an EDLR, has overcome the uncertainty and complexities in dynamics of the robot. Swift calculations, high performance and efficiency, robustness, and guaranteed stability are the main merits of the proposed method. Comparatively, the higher performance of the method is validated showing less tracking error. At the same time, greater efficiency is achieved through brief calculations, smaller control signal (voltage), and reduced power consumption leading to smaller motor sizing. In addition, the most significant advantages of the method are the independent joint structure, simplicity of design, and ease of implementation. The method has been compared with two others, namely an adaptive robust sub-controller, and a Taylor-series based robust controller through simulations. The results of simulations and comparisons have confirmed the aforementioned merits.

References

[1] F. Molteni, G. Gasperini, G. Cannaviello, and E. Guanziroli, "Exoskeleton and End-Effector Robots for Upper and Lower Limbs Rehabilitation: Narrative Review," PM&R, Vol. 10, No. 9S2, pp. 174-188, Sep. 2018.

[2] JK. Mohanta, S. Mohan, P. Deepasundar, and R . Kiruba-Shankar, "Development and control of a new sitting-type lower limb rehabilitation robot," Comput Electr Eng, Vol. 67, pp. 330-347, Apr. 2017.

[3] SF. Atashzar, M. Shahbazi, and R. V. Patel, "Haptics-enabled Interactive NeuroRehabilitation Mechatronics: Classification, Functionality, Challenges and Ongoing Research," Mechatronics, Vol. 57, pp. 001-019, Feb. 2019.

[4] W. Meng, Q. Liu, Z. Zhou, Q. Ai, B. Sheng, and SS. Xie, "Recent development of mechanisms and control strategies for robot-assisted lower limb rehabilitation," Mechatronics, Vol. 31, pp. 132-145, Oct. 2015.

[5] H. Huang, DL. Crouch, M. Liu, GS. Sawicki, and D. Wang, "A Cyber Expert System for Auto-Tuning Powered Prosthesis Impedance Control Parameters," Ann Biomed Eng, Vol. 44, pp. 1613-1624, Sep. 2015.

[6] H. Erdogan, Y. Palaska, E. Masazade, D. Erol Barkana, and HK. Ekenel, "Vision-based game design and assessment for physical exercise in a robot-assisted rehabilitation system," IET Comput Vis, Vol. 12, No. 1, pp. 059-068, Feb. 2018.

[7] E. Akdoğan, ME. Aktan, AT. Koru, M. Selçuk Arslan, M. Atlıhan, and B. Kuran, "Hybrid impedance control of a robot manipulator for wrist and forearm rehabilitation: Performance analysis and clinical results," Mechatronics, Vol. 49, pp. 077-091, Feb. 2018.

[8] SM. Ahmadi, and M. M. Fateh, "Robust control of electrically driven robots using adaptive uncertainty estimation," Comput Electr Eng, Vol. 56, No. C, Nov. 2016.

[9] E. Akdoğan, and MA. Adli, "The design and control of a therapeutic exercise robot for lower limb rehabilitation: Physiotherabot," Mechatronics, Vol. 21, No. 3, pp. 509-522, Apr. 2011.

[10] J. Wu, J. Gao, R. Song, R. Li, Y. Li, and L. Jiang, "The design and control of a 3DOF lower limb rehabilitation robot," Mechatronics, Vol. 33, pp. 013-022, Feb. 2016.

[11] M. M. Fateh, and V. Khoshdel, "Voltage-based adaptive impedance force control for a lower-limb rehabilitation robot," Adv Robot, Vol. 29, No. 15, pp. 961-971, Apr. 2015.

[12] S. Mohan, JK. Mohanta, S. Kurtenbach, J. Paris, B. Corves, and M. Huesing, "Design, development and control of a 2PRP-2PPR planar parallel manipulator for lower limb rehabilitation therapies," Mech Mach Theory, Vol. 112, pp. 272-294, Jun. 2017.

[13] M.M. Fateh, "On the Voltage-Based Control of Robot Manipulators," Int J Control Autom Syst, Vol. 6, pp. 702-712, 2008.

[14] S. Fateh, and M. M. Fateh, "Adaptive Fuzzy Control of Robot Manipulators with Asymptotic Tracking Performance," J Control Autom Electr Syst, Vol. 31, pp. 052-061, Oct. 2019.

[15] M. M. Fateh, and S. Khorashadizadeh, "Optimal robust voltage control of electrically driven robot manipulators," Nonlinear Dyn, Vol. 70, No. 2, pp. 1445-1458, Oct. 2012.

[16] S. Khorashadizadeh, and M. M. Fateh, "Uncertainty estimation in robust tracking control of robot manipulators using the Fourier series expansion," Robotica, Vol. 35, No. 2, pp. 310-336, Feb. 2017.

[17] R. Shanmugasundram, K. M. Zakaraiah, and N. Yadaiah, "Effect of parameter variations on the performance of direct current (DC) servomotor drives," JVC/Journal Vib Control, Vol. 19, No. 10, pp. 1575-1586, Jul. 2013.

[18] S. Khorashadizadeh, and M. Sadeghijaleh, "Adaptive fuzzy tracking control of robot manipulators actuated by permanent magnet synchronous motors," Comput Electr Eng, Vol. 72, pp. 100-111, Nov. 2018.

[19] M. M. Fateh, and S. Khorashadizadeh, "Robust control of electrically driven robots by adaptive fuzzy estimation of uncertainty," Nonlinear Dyn, Vol. 69, No. 3, pp. 1465-1477, Aug. 2012.
[20] A. Izadbakhsh, P. Kheirkhahan, and S. Khorashadizadeh, "FAT-Based Robust Adaptive Control of Electrically Driven Robots in Interaction with Environment," Robotica, Vol. 37, No. 5, pp. 779-800, May. 2019.
[21] S. M. Ahmadi, and M.M. Fateh, "On the Taylor series asymptotic tracking control of robots," Robotica, Vol. 37, No. 3, pp. 405-427, Mar. 2019.
[22] L. Wang, Z. Du, W. Dong, Y. Shen, and G. Zhao, "Intrinsic sensing and evolving internal model control of compact elastic module for a lower extremity exoskeleton," Sensors (Switzerland), Vol. 18, No. 3, Mar. 2018.
[23] S. M. Hashem Zadeh, S. Khorashadizadeh, M. M. Fateh, and M. Hadadzarif. "Optimal sliding mode control of a robot manipulator under uncertainty using PSO," Nonlinear Dyn, Vol. 84, No. 4, Feb. 2016.
[24] M. M. Fateh, "Robust control of flexible-joint robots using voltage control strategy," Nonlinear Dyn, Vol. 67, pp. 1525–1537, Jan. 2012.
[25] M. Jalaeian-F, M. M. Fateh, and M. Rahimiyan, "Optimal Predictive Impedance Control in the Presence of Uncertainty for a Lower Limb Rehabilitation Robot," J Syst Sci Complex, Vol. 33, No. 3, Jun. 2020.
[26] M. Jalaeian-F, M. M. Fateh, and M. Rahimiyan, "Bi-Level Adaptive Computed-Current Impedance Controller for Electrically Driven Robots," Robotica, Published online, 28 May 2020, pp. 1-17.
[27] C. Guo, S. Guo, J. Ji, and F. Xi, "Iterative Learning Impedance for Lower Limb Rehabilitation Robot," J Healthc Eng, Vol. 2017, Article ID 6732459, 9 pages, Aug. 2017.
[28] J. F. Veneman , R. Kruidhof, E. E. G. Hekman, R. Ekkelenkamp, E. H. F. Van Asseldonk, and H. Van Der Kooij, "Design and evaluation of the LOPES exoskeleton robot for interactive gait rehabilitation," IEEE Trans Neural Syst Rehabil Eng, Vol. 15, No. 3, pp. 379-386, Sep. 2007.
[29] G. A. Turley, M.A. Williams, R.M. Wellings, and D.R. Griffin, "Evaluation of range of motion restriction within the hip joint," Med Biol Eng Comput, Vol. 51, No. 4, pp. 467-477, Dec. 2012.
[30] H. Fasih, S. Tavakoli, J. Sadeghi, and H. Torabi, "Kalman Filter-Smoothed Random Walk Based Centralized Controller for Multi-Input Multi-Output Processes," Int J Ind Electron Control Optim, Vol. 2, No. 2, pp. 155-166, Spr. 2019.
[31] M. Jalaeian-F, M.M. Fateh, and M Rahimiyan, "Internal Model Impedance Control for a Lower Limb Rehabilitation Robot in the Presence of Uncertainty," 26th Iran. Conf. Electr. Eng. ICEE 2018, Mashhad, Iran: IEEE, Vol. 2018, pp. 930-935, 2018.
[32] M. Jalaeian-F, M. M. Fateh, and M. Rahimiyan, "Dynamic-Growing Fuzzy-Neural Acceleration-Based Impedance Controller for a Lower Limb Rehabilitation Robot," Electr Eng (ICEE), Iran Conf 2018, Vol. 2018, pp. 1000-1004, 2018.

Mohsen Jalaeian-F received the M.Sc. degree of control engineering from the Ferdowsi University of Mashhad, Iran, in 2012. Currently, he is a Ph.D. candidate at Shahrood University of Technology. He is also with the Center of Excellence on Soft Computing and Intelligent Information Processing (SCIIP). His research interests include robotics, control, optimization, AI/ML (soft-computing), fuzzy logic, and deep reinforcement learning.

Mohammad Mehdi Fateh received his B. Sc. degree from Isfahan University of Technology in 1988. He received his M.Sc. degree in electrical engineering from Tarbiat Modares University, Iran in 1991, and his Ph.D. degree in robotic engineering from Southampton University, the UK in 2001. He is a full professor with the Department of Electrical and Robotic Engineering at Shahrood University of Technology, Iran. His research interests include nonlinear, robust and fuzzy control, robotics and intelligent systems, mechatronics, and automation.

Morteza Rahimiyan received the B.Sc. degree from the Isfahan University of Technology, Isfahan, Iran, in 2003, and the M.Sc. and Ph.D. degrees (with honors) from the Ferdowsi University of Mashhad, Mashhad, Iran in 2006 and 2011, respectively, all in electrical engineering. He is currently an associate professor at Shahrood University of Technology, Shahrood, Iran. His research interests include operation, planning, and economics of power systems, as well as optimization.